JOURNAL OF MATERIALS SCIENCE 20 (1985) 3027–3033

Humidity sensor using sintered zircon with alkali-phosphate

Y. SADAOKA, Y. SAKAI
Department of Industrial Chemistry, Faculty of Engineering, Ehime University, Bunkyo-cho, Matsuyama, Ehime 790, Japan

A ceramic humidity sensor using alkali phosphate (tribasic), phosphoric acid and zircon as raw materials was studied. The ceramic body prepared by doping with sodium phosphate consists of zircon, Nasicon and probably glassy sodium polyphosphate. The sensitivity for humidity can be improved by doping with sodium phosphate and phosphoric acid. The specimen in which the mole ratio (Na/P) is nearly equal to one is desirable for a humidity sensor with respect to sensitivity, and the impedance is $2 \times 10^6\ \Omega$ cm or below in a dry atmosphere. The formation of Nasicon explains the decrease of impedance in the low humidity region and a decrease of impedance in the high humidity region can be achieved by the formation of sodium polyphosphate.

1. Introduction

It is well-known that the impedance of sintered porous oxide is increased considerably when it is placed in a container and then dried. The change of impedance has been ascribed to the removal of adsorbed water from the porous oxide. This observation has led to a study of some of the electrical properties of oxides in atmospheres of varying relative humidity. Recently, humidity detection and control have been very important for medical and industrial equipment, etc. In humidity sensors using porous oxides, the admittance is usually enhanced by physisorption and/or capillary condensation of water [1–4] and the protons dissociated from the adsorbed water and/or hydroxide formed on the surface are probably the dominant carriers.

Porous oxide is a material adequate for a conventional humidity sensing device which requires mechanical and chemical stability. However, the usual metal oxide has some disadvantages; the impedance is $10^8\ \Omega$ cm or more in the low humidity region and so it is difficult to detect humidity variation by using a conventional impedance meter. The impedance also increases continually with age when exposed to humid atmosphere.

In order to overcome the disadvantages, the doping of a mobile alkali ion such as lithium, sodium and potassium into a porous metal oxide was considered.

This paper presents the results of a study of the humidity sensitivity of sintered zircon with alkali-phosphate.

2. Experimental details

2.1. Materials

Fine particle zircon, alkali-phosphate (tribasic) and phosphoric acid were used. The raw materials were weighed in the prescribed mole ratio and mixed using water as a mixing medium. After the water was evaporated, the mixed powder was pressed into a disc, dried at 350° C for 12 h and finally sintered at 1000° C in air. The ceramic body obtained was then shaped to 0.05 cm × 0.8 cm × 0.8 cm. Next, RuO_2 electrodes, 0.2 cm diameter, were applied to opposite faces of the ceramic body by printing and heating at 800° C. Preparation conditions with respect to composition are summarized in Table I.

0022–2461/85 $03.00 + .12

TABLE I Components of starting materials

Specimen	Raw materials (mol)				
	$ZrSiO_4$	H_3PO_4	Na_3PO_4	Li_3PO_4	K_3PO_4
ZP	1	0.47			
ZPNa10	1	0.47	0.10		
ZPNa20	1	0.47	0.20		
ZPNa33	1	0.47	0.33		
ZPNa50	1	0.47	0.50		
ZNa10	1		0.10		
ZNa20	1		0.20		
ZNa33	1		0.33		
ZPLi10	1	0.47		0.10	
ZPLi20	1	0.47		0.20	
ZPK10	1	0.47			0.10
ZPK20	1	0.47			0.20

Polymerized sodium phosphate was prepared by fusion of a mixture of sodium phosphate and phosphoric acid at about 900° C. The polymer dissolved in water and was impregnated into a substrate already fitted with one pair of gold electrodes. The obtained specimen was finally dried at 150° C.

2.2. Measurements

The crystalline phases were identified at room temperature by standard X-ray diffraction techniques. The microstructure was examined by scanning electron microscopy and the pore size distribution was examined by means of mercury penetration porosimetry. The specific surface area was determined by the BET method using N_2 as a sorbate. A quartz spring balance was used to obtain the adsorption-isotherm for H_2O.

Humidity–impedance characteristics were measured with an LCZ meter (10^2 to 2×10^4 Hz). Humidities (p/p_0), ranging from 0 to 0.9, were prepared by mixing dry and moist air in controlled proportions in the temperature range 20 to 60° C.

3. Results and discussion

3.1. Microstructure and porosities

The surfaces of the specimens were observed by SEM. The microstructures of the specimens with and without sodium phosphate are shown in Fig. 1. In the sodium-free specimen, distinct sintering could not be observed (Fig. 1a). In contrast, the specimen with a sodium-additive (ZPNa10) had small new particles formed on the larger particles (Fig. 1b) and fewer of the small particles and more glass phases were confirmed in the specimen with more of the sodium additive (Figs. 1c and d).

TABLE II Characteristic values for sintered oxide

Specimen	Pore radius (10^{-5} cm)	Pore volume ($cm^3 g^{-1}$)	S_{N_2}* ($cm^2 g^{-1}$)	W_{H_2O}† ($g g^{-1}$)
ZP	1.4	0.1	4.0×10^4	0.011
ZPNa10	4.0	0.034	0.6×10^4	0.0072
ZPNa20	5.0	0.005	0.2×10^4	0.001
ZPNa33	5.0	0.021	0.2×10^4	–

*Surface area.
†Amount of adsorbed water at $p/p_0 = 0.9$.

The pore-size distribution of the specimens measured by mercury penetration porosimetry is shown in Fig. 2. The average pore radius and pore volume in the sodium-free specimen (ZP) were estimated to be about 1×10^{-5} cm and 0.1 $cm^3 g^{-1}$, respectively. It was found that the pore volume for the specimens containing sodium was much smaller than that of the sodium-free specimen. The characteristic values for each sample are summarized in Table II with the surface area determined by the BET method using nitrogen as a sorbate.

Water sorption was measured gravimetrically using a quartz spring balance. The amounts of adsorbed water at $p/p_0 = 0.9$ for the oxides are summarized in Table II. It was confirmed that the amount of adsorbed water on the specimens with sodium additive was much smaller than that on the sodium-free specimen.

The X-ray diffraction patterns of the specimens with sodium phosphate and phosphoric acid indicated a new phase formation which could not be confirmed for the sodium-free specimen. It is expected that the reactants obtained from a three-component mixture by a high temperature reaction are Nasicon ($Na_{1+x}Zr_2Si_xP_{3-x}O_{12}$) and sodium polyphosphate. Although ASTM data for Nasicon are still absent, the X-ray diffraction patterns have been reported by von Alpen *et al.* [5] and Yoldas and Lloyd [6]. For Nasicon, the X-ray diffraction peaks appeared at $d = 0.2895$ nm and other d spacings. In addition, the distinct peaks for $ZrSiO_4$ appeared at $d = 0.4434$, 0.3302 and 0.2518 nm. The intensity ratio of each peak is summarized in Table III. It is clear that the formation of Nasicon is confirmed by the ZPNa system but not for the ZNa and Z systems. For all the samples, the main component is $ZrSiO_4$

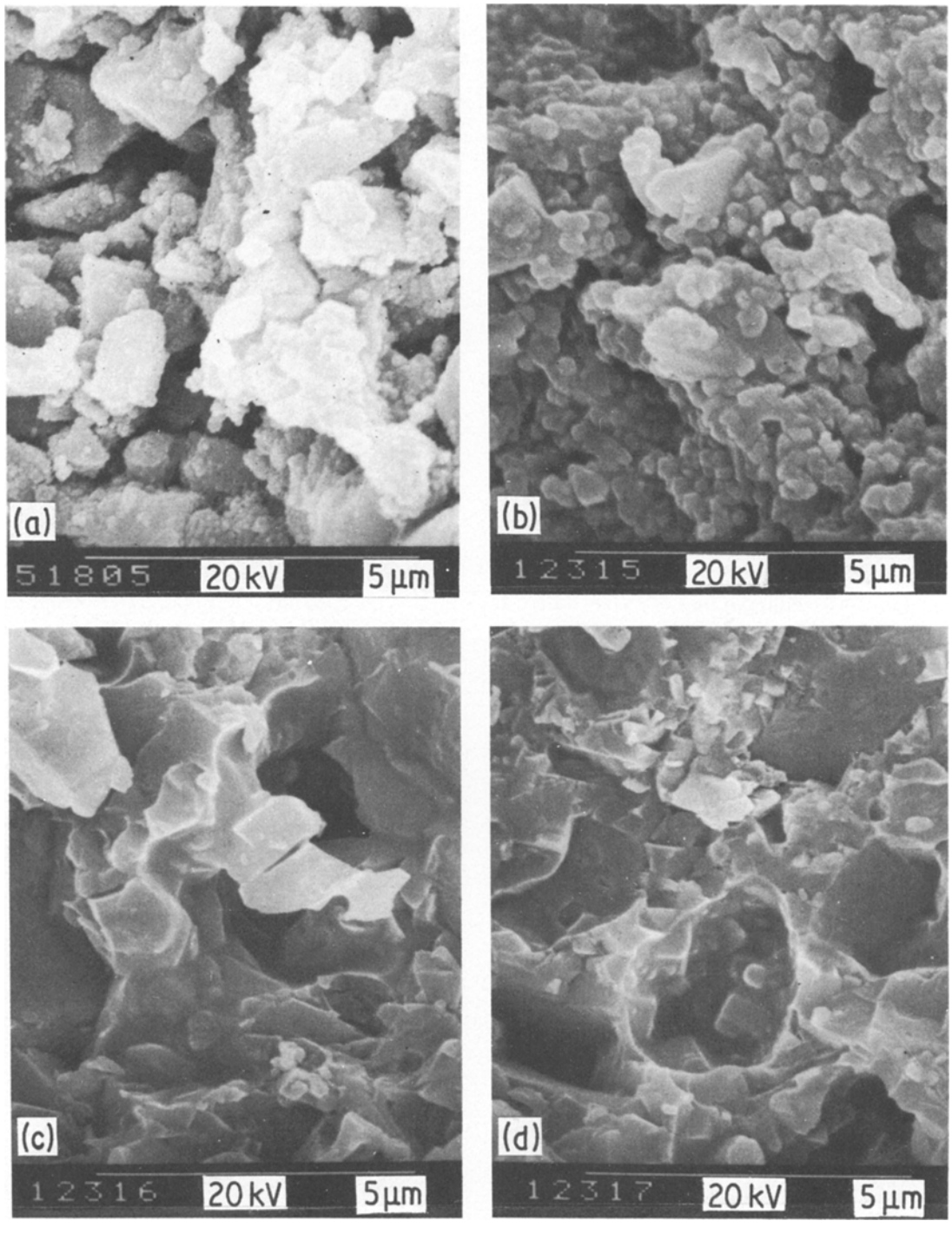

Figure 1 Scanning electron micrographs of: (a) ZP; (b) ZPNa10; (c) ZPNa20; (d) ZPNa33.

and this result is easily recognized in the SEM (Fig. 1). In addition, it seems that the Nasicon phase is formed on the surface of the $ZrSiO_4$ particle.

As mentioned above, the existence of the glass phase is confirmed by SEM. This layer, which appeared with an increase of sodium phosphate, seemed to be composed mainly of linearly polymerized sodium phosphate although a detailed analysis has not been carried out.

TABLE III Intensity of X-ray diffraction patterns

Specimen	$ZrSiO_4$		Nasicon
	0.4434 nm	0.2518 nm	0.2895 nm
Z	62	100	0
ZP	77	100	0
ZPNa10	67	100	14
ZPNa20	75	100	40
ZPNa33	77	100	35
ZNa10	60	100	0
ZNa33	58	100	0

3.2. Impedance

Fig. 3 shows the humidity–impedance characteristics for ZP, ZNa10 and ZNa20. The distinct decrease in the impedance could not be achieved by the sodium phosphate doping method in a dry atmosphere ($p/p_0 = 0$), while the decrease could be achieved in a humid atmosphere. For the specimens with alkali phosphate and phosphoric acid, the distinct decrease in the impedance was achieved in a dry atmosphere as shown in Fig. 4. The impedance in the dry atmosphere was in the order of ZPNa20 < ZPK20 < ZPLi20. From these observed results, it is confirmed that the impedance in a dry atmosphere can be effectively decreased by doping with both sodium phosphate and phosphoric acid. Fig. 5 shows the humidity–impedance relations for ZPNa specimens with different concentrations of sodium. For ZPNa with $0.5 < Na/P < 1.33$ especially, the impedance is $2 \times 10^7\ \Omega$cm or below in the low humidity region; thus, it was realized that these specimens had good humidity–impedance characteristics to detect humidity in an atmosphere using a conventional impedance meter. For the series of ZPNa, the response of the specimens was assessed by making rapid changes from 0.4 to 0.8 and the reverse. The response time was estimated to be

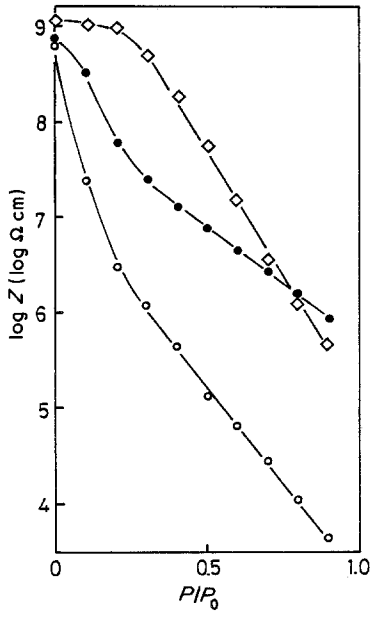

Figure 3 Humidity dependence of impedance at 30° C, applied frequency 100 Hz: ◊, ZP; ●, ZNa10; ○, ZNa20.

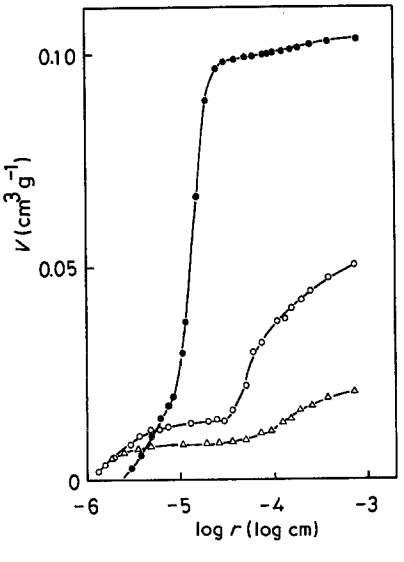

Figure 2 Pore radius dependence of pore volume: (●) ZP; (○) ZPNa20; (△) ZPNa33.

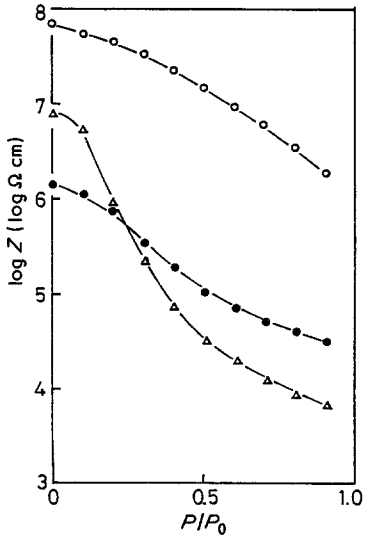

Figure 4 Humidity dependence of impedance at 30° C, applied frequency 100 Hz: ○, ZPLi20; ●, ZPNa20; △, ZPK20.

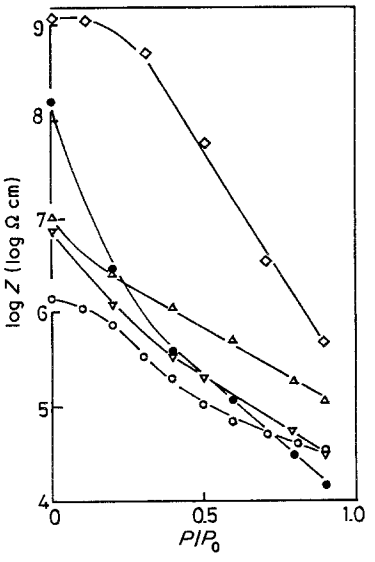

Figure 5 Humidity dependence of impedance at 30° C, applied frequency 100 Hz: ◊, ZP; △, ZPNa10; ○, ZPNa20; ▽, ZPNa33; ●, ZPNa50.

within 120 sec for all the specimens in the humidification and desiccation processes.

The temperature dependence of impedance for some specimens under nitrogen atmosphere is shown in Fig. 6. For all specimens, the temperature dependence of impedance can be expressed as

$$Z = Z_0 \exp(E/kT) \quad (1)$$

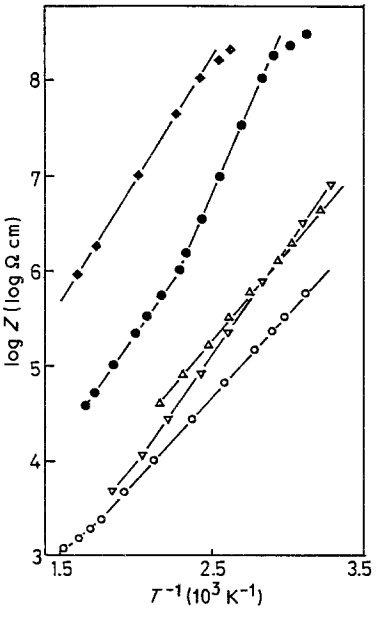

Figure 6 Temperature dependence of impedance in nitrogen atmosphere. ♦, ZPLi10; △, ZNPa10; ○, ZPNa20; ▽, ZPNa33, ●, ZPNa50.

where Z_0 is the pre-exponential factor, E the activation energy, k the Boltzmann constant and T the absolute temperature.

For ZPNa20, the activation energies for impedance were estimated from the curve to be 0.34 eV for temperatures lower than 250° C and 0.21 eV for the high temperature region. The observed values are comparable to the literature values of about 0.36 and 0.21 eV for Nasicon ($Na_3Zr_2Si_2PO_{12}$) [5], respectively. In addition, ZPNa20 has a resistivity of 6×10^3 Ω cm which is higher than that for Nasicon (10 Ω cm) at 250° C. From these observed results and the results of the X-ray diffraction patterns, it is concluded that the highly conductive Nasicon layer is formed on the surface of the $ZrSiO_4$ particle. The impedance for ZPNa10 is higher than that for ZPNa20, while the activation energy is comparable. This difference of the impedance is caused by the limited amount of the Nasicon phase.

It is well known that Nasicon is a highly conductive compound with three-dimensional framework structures containing tunnels in which mobile sodium ions are located. Although similar framework structures may be formed for ZPLi10, the activation energy and impedance for ZPLi10 are higher than those for ZPNa10. This discrepancy can be realized by the difference in the ionic potential for the mobile alkali ions.

For the ZPNa species, the increases in impedance and activation energy with a sodium concentration in the range of Na/P > 1.0 (ZPNa50 > ZPNa33 > ZPNa20) were observed in a dry atmosphere, while the X-ray diffraction peaks assigned to Nasicon were confirmed in all samples. This variation with sodium concentration may be caused by the existence of excess sodium phosphate since the decrease in the impedance for $ZrSiO_2$ could not be achieved by the sodium phosphate doping method in a dry atmosphere as shown in Fig. 3.

The relationship between the impedance and the mole ratio of sodium and phosphorus (N/P) in the raw materials is shown in Fig. 7. For ZPNa specimens, a decrease in impedance with sodium concentration in the range of Na/P ⩽ 1 was observed in all humidity regions. Fig. 8 shows the humidity dependence of the activation energy for ZPNa specimens. For ZPNa10, ZPNa20 and ZPNa33, the activation energy is

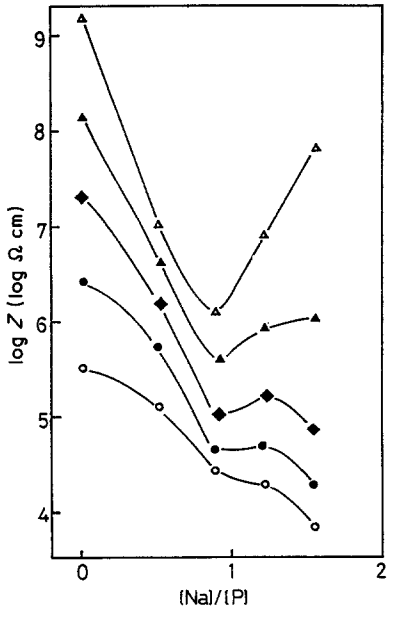

Figure 7 Relationship between impedance and ratio of sodium and phosphorus for the ZPNa system. Humidity: △, 0.0; ▲, 0.2; ♦, 0.4; ●, 0.6; ○, 0.8.

comparable to the literature value for Nasicon, thus, it seems that the product formed on the particle surfaces is mainly composed of a highly conductive Nasicon.

Recently, it was confirmed that the bulk resistance for porous $Na_2Zr_2SiP_2O_{12}$ and $Na_3Zr_2Si_2PO_{12}$ was poorly dependent on the humidity and the humidity dependence of the

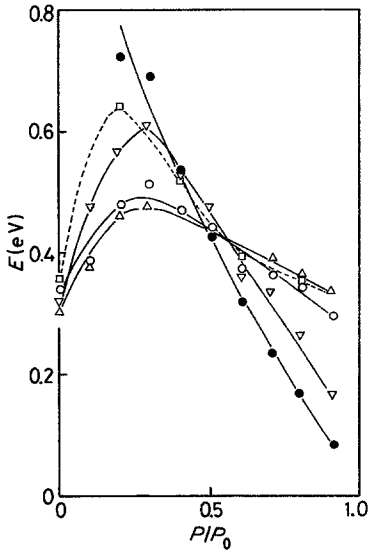

Figure 8 Humidity dependence of activation energy for the ZPNa system: △, ZPNa10; ○, ZPNa20; ▽, ZPNa33; ●, ZPNa50; □, $Na_2Zr_2SiP_2O_{12}$.

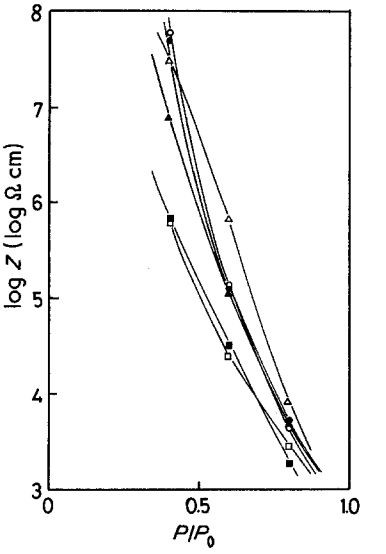

Figure 9 Humidity dependence of impedance for sodium polyphosphate film. Na/P: ●, 1.4; ○, 1.2; △, 1.0; ▲, 0.9; □, 0.6; ■, 0.4.

resistance for the specimens was interpretable in terms of the increase in the surface conductance by water sorption [7]. For comparison, the activation energy of resistance for porous $Na_2Zr_2SiP_2O_{12}$ is shown in Fig. 8. It is clear that the humidity dependence of the activation energy for ZPNa10 and ZPNa20 is similar to that for porous $Na_2Zr_2SiP_2O_{12}$. From these obtained results, it is concluded that the impedance decrease with humidity is interpretable in terms of proton conduction which is enhanced by the formation of a physisorbed water layer on the surfaces. In addition, the initial and successive decrease in the activation energy with humidity is interpretable in terms of the parallel contribution of the conductance of the Nasicon layer and the humidity dependent surface conductance.

On the other hand, it seems that the surface layer for ZPNa50 is composed of a highly conductive Nasicon and linearly polymerized sodium phosphate and the Nasicon layer may be wrapped with sodium phosphate polymer since the increase in impedance with a sodium concentration in the range of Na/P > 1 was observed in a dry atmosphere. In addition, the existence of through pores is not appreciably found in ZPNa33 as shown in Fig. 1d. Thus, it is expected that the decrease in the impedance with humidity is caused by the water sorption in sodium polyphosphate. To confirm this

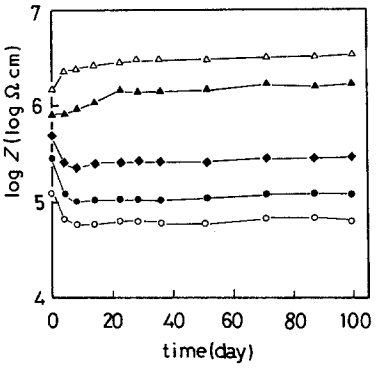

Figure 10 Impedance changes for ZPNa20 after storage in room conditions. Humidity: △, 0.0; ▲, 0.2; ♦, 0.4; ●, 0.6; ○, 0.8.

expectation, the humidity dependence of impedance for a sodium polyphosphate film was measured as shown in Fig. 9. For all specimens, the distinct humidity dependence of impedance is observed. In addition, it is confirmed that the impedance for a sodium polyphosphate film is $10^8\,\Omega$ or more which is higher than that ($\approx 10^5\,\Omega$) for a $Na_2Zr_2SiP_2O_{12}$ film in low humidity region.

Finally, the sensor durability in room conditions is shown in Fig. 10 for ZPNa20. Although, a change in sensitivity was observed in the initial periods, after this period, the sensitivity did not change during 100 days or more. For ZNa, ZPLi and ZPK specimens, the impedance decreases continually with age and stable sensitivity cannot be observed.

References

1. T. NITTA, *Ind. Eng. Chem. Prod. Res. Dev.* **20** (1981) 669.
2. F. UCHIKAWA, K. MIYAO and K. SHIMAMOTO, *Oyo Butsuri* **52** (1983) 451.
3. Y. SHIMIZU, H. ARAI and T. SEIYAMA, *Denki Kagaku* **50** (1982) 831.
4. Y. SADAOKA and Y. SAKAI, *ibid.* **51** (1983) 437.
5. U. VON ALPEN, M. F. BELL and W. WICHELHANS, *Mat. Res. Bull.* **14** (1979) 1317.
6. B. E. YOLDAS and I. K. LLOYD, *Mat. Res. Bull.* **18** (1983) 1171.
7. Y. SADAOKA and Y. SAKAI, *Denki Kagaku* in press.

Received 1 October
and accepted 2 November 1984